

Analysis of Particle Rearrangement during Sintering by Micro Focus Computed Tomography (μ CT)

M. Nöthe^{1,a}, M. Schulze^{2,b}, R. Grupp^{1,c}, B. Kieback^{1,d}, A. Haibel^{3,e} and J. Banhart^{3,f}

¹Institute of Material Science, Technische Universität Dresden, Germany

²Institute of Photogrammetry and Remote Sensing, Technische Universität Dresden, Germany

³Structural Research, Hahn-Meitner-Institut Berlin, Germany

^amichael.noethe@tu-dresden.de, ^bmatthias.schulze@tu-dresden.de, ^crainer.grupp@hmi.de, ^dbernd.kieback@ifam-dd.fraunhofer.de, ^ehaibel@hmi.de, ^fbanhart@hmi.de

Keywords: sintering, cooperative material transport, tomography, image analysis

Abstract. The decrease of the distance between particle centers due to the growth of the sinter necks can be explained by the well known two-particle model. Unfortunately this model fails to provide a comprehensive description of the processes for 3D specimens. Furthermore, there is a significant discrepancy between the calculated and the measured shrinkage because particle rearrangements are not considered. Only the recently developed analysis of the particle movements inside of 3D specimens using micro focus computed tomography (μ CT), combined with photogrammetric image analysis, can deliver the necessary experimental data to improve existing sintering theories. In this work, μ CT analysis was applied to spherical copper powders. Based on photogrammetric image analysis, it is possible to determine the positions of all particle centers for tracking the particles over the entire sintering process and to follow the formation and breaking of the particle bonds. In this paper, we present an in-depth analysis of the obtained data. In the future, high resolution synchrotron radiation tomography will be utilized to obtain in-situ data and images of higher resolution.

Introduction

The two-particle model is used to describe the initial stages of the sintering process as growth of interparticle contacts. In this model, the material diffusion leads to the decrease of distance between particle centers, the minimization of free surface energy and homogenous shrinkage of macroscopic samples [1, 2, 3, 4]. When additional materials are transported, this model is no longer capable of describing the shrinkage of macroscopic specimens. Thus, to improve the theoretical description of sintering, cooperative material transport processes (movements of entire particles for example rotations) need to be described by a mathematical model [1, 5, 6]. Rotations can be caused by:

- The desire to form low energy grain boundaries in the interparticle contact zones [7],
- Tensions [8] caused by inhomogeneous particle center approach due to different particle sizes and inhomogeneous packings and
- Asymmetric [8] tensions inflicted by asymmetric sintering necks.

The cooperative material transport processes can significantly contribute or even dominate the sintering process as observed in particle rows, 2D samples and on the surface of three dimensional specimens. Currently, the high resolution computer tomography combined with advanced methods of photogrammetry is the only available method for observing and quantifying cooperative material transport processes inside of 3D specimens [9, 10]. In the future, the obtained data will help improve existing sintering theories and computer simulations (e.g. [11, 12]).

Experiments

The specimens used consisted of air atomized copper powder (ECKA Granulate AK 0.1...0.125 mm). To meet the requirements of image analysis and obtain ideally spherical particles of 100...120 μm, the powder was sieved and subsequently rolled over a slightly inclined (5 °) glass panel. Specimens of 9,000...10,000 particles were prepared by filling the copper powder into aluminum oxide crucibles. When the cone beam tomography was used, several reference points (6 cuts by a diamond wire saw in the crucibles) were taken to measure the precise voxel size in each 3D image (903 * 903 * 903 voxels of approximately 5 μm). Optimal 3D images were obtained by increasing the power voltage to 175 KV, obtaining 1440 projection images and using a 0.8 mm copper filter between tube and sample to adjust the X-ray spectrum (see [9] for further details on our tomography setup and the image processing). To fix the particles in their positions, the specimens were subjected to a pre-sintering step in a hydrogen atmosphere prior to the first analysis by micro focus computer tomography. The stages of sintering were selected based on dilatometer measurements and expert judgments from prior experience:

- a temperature series (specimen 1) with 600 (pre-sintering), 700, 800, 900, 1000 and 1050 °C sintering temperature and no dwell time (heating rate 5 K/min)
- a time series (specimen 2) prepared at 1050 °C with dwell times of 0 (pre-sintering), 5, 10, 20, 40, 80, 160 and 320 minutes (heating rate 5 K/min).

The sintering stages were frozen by cooling down the samples to room temperature.

In the first step of the image analysis, all particles in the specimen were identified. With the rough estimation of the position of the particle positions, accurate locations of surface points of the respective particle could be obtained, and by fitting a sphere function through the surface points, the accurate position of the particle center was determined. Furthermore, the particles could be easily tracked throughout the entire sintering process (0.5 % or less of the particles were either not

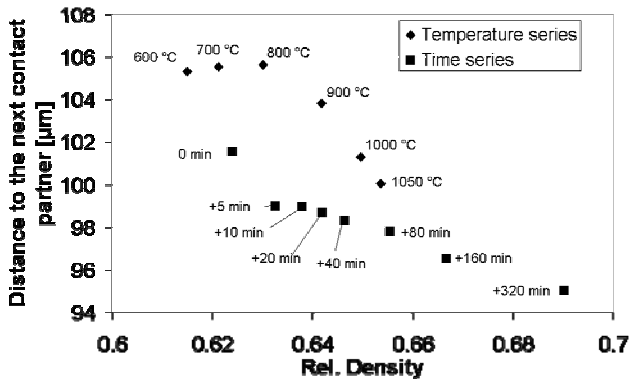


Fig. 1: Contribution of particle center approach to densification

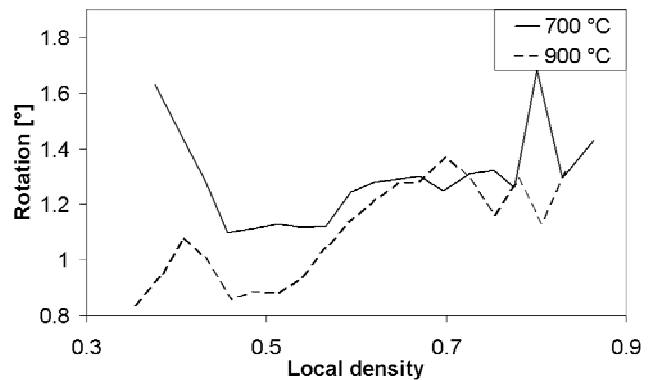


Fig. 2: Differential rotation of the temperature series sample vs. the local density

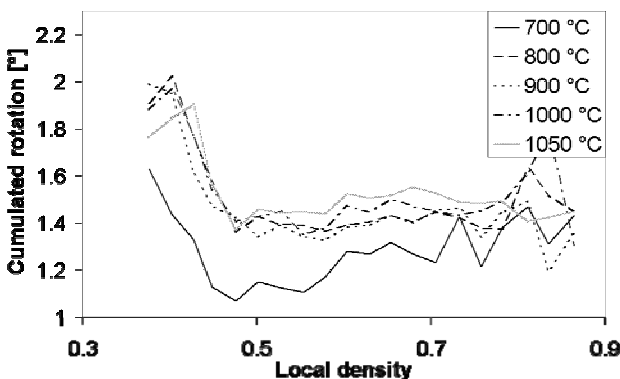


Fig. 3: Cumulated rotations in specimen 1 vs. local density

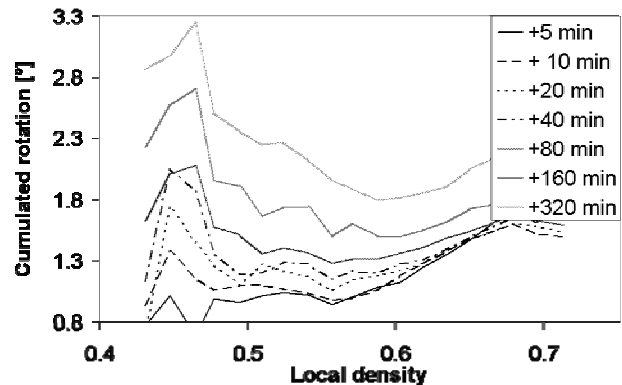


Fig. 4: Cumulated rotations in the time series specimen vs. local density

tracked over the process or inadequate for the particle center measurement), and all inter particle contacts could be determined.

Next, the results of image analysis were subjected to an extensive statistical evaluation in order to identify relations between the measured parameters. The sphere of influence of each particle was determined by the Voronoi tessellation of the dataset. The numbers of new and broken contacts were determined.

In this study, we focus mainly on particle rotation. The rotation was determined by calculating the changes of angles in all particle triplets, which were connected after the pre-sintering step and after the sintering step of interest (i.e., the cumulative rotation was determined). To measure the contribution of the particle center approach to the sintering process as described by the two particle model, we calculated the distance between contacting particles.

To exclude the edge effects for the following statistical analysis all edge particles and 4 additional particle layers were excluded from the data analysis. To determine the local density within the neighborhood of a particle the volume of the Voronoi cells within the respective specimen region was divided by the volume of the particles within the region.

Results

Figure 1 shows the average distance between next coordination partners for all investigated sintering stages plotted versus the sample density. Obviously, a continuous densification of the specimens occurs. Looking at the temperature series specimen, no particle center approach is observed below 900 °C. Thus, the observed densification below 900 °C is believed to be attributed to the cooperative material transport processes and the densification due to particle center approach as described by the two particle model can be ruled out. At higher temperatures, the contribution of the particle center approach can always be detected. In addition to the directly measured densification, the coordination number increases over the entire sintering process. This observation, along with the verification of new and broken contacts, means that particle rearrangements must occur.

Figure 2 shows the differential rotation (i.e. the change of angles in connected particle triplets between two subsequent sintering stages) in the temperature series specimen during the first and third sintering steps. In almost all stages of the sintering process, the differential rotation is smaller than the detection threshold for rotations. The differential rotation *computed* for the sintering step at 900 °C is plotted as a *representative graph of the detection threshold* of the measured rotations with respect to the local density. In regions with low local density, the detection threshold is roughly 0.9 °. It increases to values above 1.5 ° for regions with high density as in these regions the number of surface points applicable for the fit of the sphere model is much reduced. This results in less accurate determination of the particle center positions.

The first two sintering steps (600 °C and 700 °C) are the only sintering steps where rotations exceed the detection threshold for low local densities (However, the rotation during sintering at 700 °C is only marginally larger than the detection threshold). This means that during the first stages of sintering, extensive rotations occur and the driving force is significantly reduced. In regions with higher densities, the rotation is significantly inhibited by the need to push away particles in the optimal path of rotation (i.e. is effectively a counteracting force).

To overcome the problem of the high detection threshold, we measured the cumulated rotations (i.e. the change of angles in connected particle triplets between the pre-sintered stage and the respective sintering stage). Figure 3 shows the particle rotation plotted versus the local density for the temperature series specimen. The observed cumulated rotation increases with the progress of the sintering process. In regions of low local density the cumulated rotation stagnates after the sintering step at 900 °C. This stagnation of the cumulated rotation coincides with the first detectable particle center approach. At this temperature, a diversification of the interparticle contact diameters can occur which can tip the balance of the forces inflicted by all coordination partners of a particle. The most extensive cumulated rotations are observed in regions with low local densities (below 50 %) as the counteracting inhibiting force (see above) is very low. In regions with higher density

the driving force is not reduced. So it is only natural to see a slight increase in rotations in regions with higher densities during the last sintering steps.

Figure 4 shows the cumulative rotations in the time series specimen. In this specimen, a continuous rotation was observed. The largest rotations were observed in regions with low local densities as there were inhibiting forces in regions with high local density.

Conclusions

Micro focus computer tomography combined with photogrammetric image analysis is a useful tool for gathering quantitative data on cooperative material transport processes inside 3D metal powder specimens. We used for our first experiments polycrystalline copper powder of 100...120 μm diameter. During the sintering process, we were able to observe continuous particle rotations. After the sintering step at 900 °C of the temperature series that cumulative rotation no longer increases in regions of low density. This stagnation is believed to be attributed to the diversification of the interparticle contact diameters as the first detectable particle center approach was observed during the same sintering step. The need to push away particles in the path of rotation is an effective counteracting force. Thus, most extensive rotations were found to occur in regions with low local density, and moreover, the driving force depleted rapidly in these regions. In addition, the density of our specimens increased at temperatures below the first detectable particle center approach. This means that the densification must be attributed to the cooperative material transport processes.

In the current experiments, only a single crystal copper powder was used for free sintering without crucible. We are still waiting for the synchrotron CT and will set up the furnace for in-situ measurements. We expect to obtain some results in the next several months and will report them in the PM 2006.

Acknowledgements

The authors thank the ECKA Granulate GmbH & Co. KG for providing the copper powder and the DFG (Deutsche Forschungs Gemeinschaft) for their financial support in this research.

References

- [1] Geguzin, J.E.: Physik des Sinterns, VEB Deutscher Verlag für Grundstoffindustrie, Leipzig, 1973
- [2] Schatt, W.: Sintervorgänge, VDI-Verlag 1992
- [3] German, R.M.: Sintering in theory and practice, John Wiley & Sons, Inc. 1996
- [4] Exner, H.E.: Jahrbuch „Technische Keramik“, , Vulkan-Verlag, Essen 1988
- [5] Exner, H.E.: Grundlagen von Sintervorgängen. Berlin/Stuttgart: Gebrüder Borntraeger 1978
- [6] Wieters, K.P.: Korngrenzeneinfluß beim defektaktivierten Sintern; Dissertation B; TU Dresden 1989
- [7] Sutton, A.P., Balluffi R.W.: Interfaces in crystalline materials, Oxford University press 2003
- [8] Boiko, J. I., Lachtermann, R.: Poroskovaja metallurgija 8 (1976) 31
- [9] Nöthe, M., Pischang, K., Ponížil, P., Bernhardt, R., Kieback, B.: Advances in Powder Metallurgy & Particulate Materials - 2002, ISBN: 1-878954-90-3, Part 13, 176
- [10] Lame O., Bellet, D., Di Michiel, M., Bouvard, D.: Nucl. Inst. And Meth. in Phys. Res. B 200 (2003) 287 294
- [11] Redanz, P., McMeeking, R.M.: Philosophical Magazine, 83 (2003) 2693.
- [12] Olevsky, E.A.: Theory of sintering: from discrete to continuum, Mater. Sci. Eng. R23 (1998) 41